Effect of Li_2CO_3 on the properties of Portland cement paste

Hang He · Yuli Wang · Fengxia He · Shuqiong Luo · Songhui Liu

Abstract In order to increase the application of CO_2 in cementitious materials and to develop new additives for cement-based materials, the effect of lithium carbonate (Li_2CO_3) on the properties of Portland cement (PC) paste was investigated. The hydration heat of fresh paste was tested and the hydration products were characterized using XRD, TG–DTA, SEM and MIP. The results showed that both the initial and final setting time of the PC paste was prolonged with increasing Li_2CO_3 content. While, the compressive strength of the hardened PC paste at 1 day, 7 days and 28 days increased initially and then decreased. When the content of Li_2CO_3 was 0.09wt%, the initial and final setting time was increased by 19.8% and 27.7%, and the compressive strength at the age of 1 day, 7 days and 28 days was increased by 47.6%, 21.2% and 14.0%, respectively. Hydration heat, TG–DTA, XRD, SEM, pore structure and other tests showed that Li_2CO_3 promoted the formation of AFt, and prolonged the arrival time of hydrated calcium silicate peak, but increased the formation of hydrated calcium silicate. Especially when the Li_2CO_3 content was below 0.09wt%, the pore structure was also optimized. Based on the above results, when the

content of Li_2CO_3 is not greater than 0.09wt%, not only the setting of the Portland cement paste can be retarded, but also the early strength can be enhanced. This can provide a good reference for the use of Li_2CO_3 in the preparation of new Portland cement-based material admixtures.

Keywords Lithium carbonate · Portland cement · Compressive strength · Setting time · Retarder

1 Introduction

In summer or mass concrete construction, admixtures with a retarding effect are normally used in most projects for the concrete mixture to maintain plasticity for a long time. Retarders usually extend the initial and final setting time of concrete, reduce the rate of hydration heat release, and reduce slump loss, so that fresh concrete can maintain plasticity for a long time [1, 2]. Therefore, the search for retarders with better performance has always been a hot spot for scholars [3–5].

At present, the commonly used retarders include sugar-containing carbohydrates (glucose, sucrose, etc.); inorganic salts (borates, phosphates, etc.); hydroxycarboxylic acids and lignosulfonates. Scholars have extensively studied the effects of different types of retarders on the properties of cement-based materials and described the retarding mechanism

H. He · Y. Wang · F. He · S. Luo (✉) · S. Liu
Henan Key Laboratory of Materials On Deep-Earth Engineering, School of Materials Science and Engineering, Henan Polytechnic University, Jiaozuo 454003, China
e-mail: luoshuqiong@hpu.edu.cn

[6–11]. Regarding the study of carbohydrate compounds, Zhang [12] et al. reported the retarding effect of threitol, xylitol and sorbitol on Portland cement (PC), and pointed out that only the threonine diol functional group can delay the setting time. The more the number of hydroxyl groups, the more significant the effect. Sugar alcohols have no negative impact on the hydration and mechanical properties of Portland cement. Li [13] et al. found that a handful of sucrose can prolong the coagulation and hardening of the cement paste and increase the fluidity of the cement paste, while excessive sucrose can accelerate the coagulation hardening. In addition, sucrose significantly increases the compressive strength at 3 days because of the decrease of the porosity. Combrinck [14] et al. reported that glucose-based retarders can reduce the development rate of the capillary pressure in concrete, inhibit shrinkage, and reduce concrete cracking area. Some scholars also pointed out that the retarding effect of citric acid is better than glucose-based retarder [15]. Lei [16] et al. explored the effect of maltodextrin on Portland cement mortar and considered that the retarding mechanism of maltodextrin stems from the surface adsorption of cement particles, which leads to the reduction of ettringite and other products, thus prolonging the hydration reaction. The compressive strength is only improved at low content ($\leq$ 0.05%) and long age ($\geq$ 1 day).

There are also many reports on the research of inorganic salts. Ltifi [17] et al. showed that sodium tripolyphosphate can affect the early hydration of PC, and its concentration is the key factor. The higher the concentration, the greater the early hydration delay. Ramachandran [18] et al. also reported that compared with cement with an induction period of 2 h, phosphate can extend the induction period of ordinary Portland cement up to 72 h, and acid phosphate is more effective than its corresponding salt. In most cases, the degree of elongation of the induction period increases as the amount of retarder is increased. Phosphate mainly achieves the retarding effect by inhibiting the conversion of free water to chemically bound water and constrained water, and at the same time changing the production and consumption rate of α-C_2SH [19]. Borax can also inhibit the early hydration reaction rate of cement, reduce the amounts of hydration products and gel structure [20], and reduce the yield stress and plastic viscosity of the paste within an appropriate content to improve rheological properties [21]. Sodium tetraborate has been studied for the preparation of geopolymer mortar, which can prolong the setting time while reducing the drying shrinkage of the mortar, but has little effect on the strength [22].

Some scholars are committed to the research of carboxylic acid retarders and sulfonate retarders. The amphoteric polycarboxylate retarder prepared by Xu [23] et al. has higher absorptivity to cement particles than conventional polycarboxylates, and the hydration reaction is significantly prolonged. The retarder prepared by Liu [24] et al. using sulfonate has a better retardation effect on cement paste, and the rheological properties are improved, but the compressive strength of the early and later ages is reduced.

In summary, the existing commercial retarders are mostly used in liquid form, have a short shelf life, and have insufficient performance and effect. For example, borax is easily weathered in dry air. Because of its low water-reducing rate and retardation, lignin sulfonate has almost no-impact on the compressive strength of concrete. Therefore, so the application of inorganic salt retarders in concrete is limited. However, in order to further a stable and effective new retarder, the influence of Li_2CO_3 on the properties of PC paste was studied. The obtained results can provide a new reference for the application of concrete engineering.

2 Raw materials and experimental methods

2.1 Raw materials

In this study, Ordinary PC (42.5) was employed. Its main properties are shown in Table 1 and the chemical composition is shown in Table 2. Lithium carbonate is a chemical reagent, and the effective content is 99.5 wt%. Water is clean tap water.

2.2 Test methods

The water-cement ratio at 0.35 was used throughout the experiments, and lithium carbonate was incorporated at 0 wt%, 0.03 wt%, 0.06 wt%, 0.09 wt%, 0.12 wt%, and 0.15 wt% of the mass of the cement. The setting time of cement paste was measured based on the Chinese National Standard GB/T1346-2011 "Test methods for water requirement of normal

Table 1 Main properties of OPC 42.5

Cement	Fineness/%	Stability	Setting time/min		Flexural strength/MPa		Compressive strength/MPa	
			initial	final	3 d	28 d	3 d	28 d
OPC 42.5	1.6	qualified	206	338	5.7	9.2	25.5	50.1

Table 2 Chemical composition of cement/%

SiO_2	CaO	Al_2O_3	Fe_2O_3	MgO	Na_2O	K_2O	Loss
24.53	61.86	5.37	3.32	2.78	0.36	0.20	0.12

consistency, setting time and soundness of the Portland cement" [25]. The sample size for compressive strength is 40 mm × 40 mm × 40 mm. The samples were cured under the condition of 20 ± 2 °C and humidity ≥ 95%. Following this, the compressive strength at 1 day, 7 days and 28 days was examined.

The hydration heat was tested using TAM Air 8-channel hydration microcalorimeter, and the continuous process of hydration heat release of cement paste was recorded for more than 40 h.

X-ray diffraction (XRD) was adopted to examine the hydrated products. The samples subjected to different curing ages were immersed in absolute ethanol for more than 24 h, and then dried under vacuum at 40 °C. Subsequently, the dried samples were ground to a powder which can go through a 75 μm sieve. The Japanese-made Smartlab X-ray diffraction was used for this study. The XRD patterns were recorded over 2θ ranging from 5° to 70° with a scanning rate of 10° min^{-1}. TG–DTA test was carried out using the HCT-3 type microcomputer differential thermal balance made in China. The temperature was increased from 30 to 800 °C at a heating rate of 10 °C/min.

SEM morphology was observed by a German Merlin Compact field emission scanning electron microscope.

The pH value of fresh paste was examined using a pHS-25 digital pH meter.

MIP was used to characterize the pore structure of hardened samples: Prior to this, the middle part of the test block which was cured for corresponding ages was placed into a glass bottle filled with absolute ethanol and immersed for 72 h. Subsequently, the sample was separated from the absolute ethanol and dried under vacuum at 40 °C for 24 h. Finally, the dry samples were examined by AutoPore IV 9510 automatic mercury intrusion meter.

3 Results and analysis

3.1 Setting time

The setting time of the PC paste with different contents of Li_2CO_3 is shown in Fig. 1. It was observed that both the initial and the final setting time are prolonged as the content of Li_2CO_3 is increased. The initial and the final setting time of the control sample are 369 min and 434 min, respectively. The prolongation of initial setting time and final setting time is the longest when the content is 0.15 wt%. In comparison, the initial setting time of the sample with Li_2CO_3 at 0.15 wt% is increased by 47.4%. Correspondingly, the final setting time is increased by 39.2%. This shows that Li_2CO_3 has prolonged the setting of the PC paste.
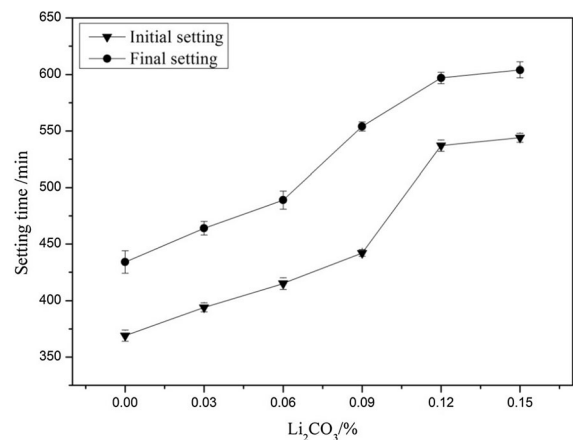
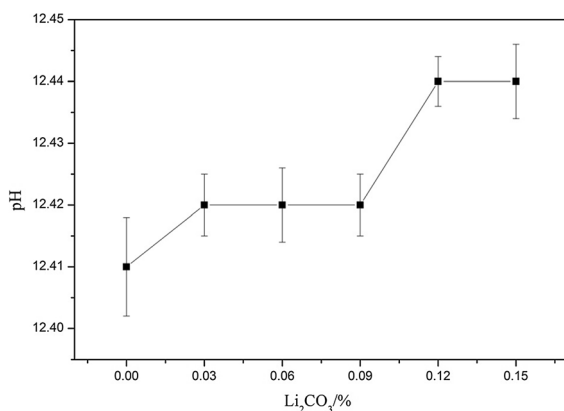**Fig. 1** The setting time of PC paste with different contents of Li_2CO_3

3.2 pH value and compressive strength

The pH value of the fresh pastes is plotted in Fig. 2, showing that the addition of Li_2CO_3 increases the pH value of the PC paste. The more the content of Li_2CO_3, the higher the pH value. When the content of Li_2CO_3 is 0.12 wt%, the pH value of the paste reaches 12.44. This may be because Li_2CO_3 reacts with $Ca(OH)_2$ in the PC paste to form LiOH. As the alkalinity of LiOH is higher than that of $Ca(OH)_2$, the OH^- ion concentration is higher in the paste with Li_2CO_3 than that in the paste without Li_2CO_3. Consequently, as the content of Li_2CO_3 is increased, the pH value of the fresh paste becomes higher and higher.
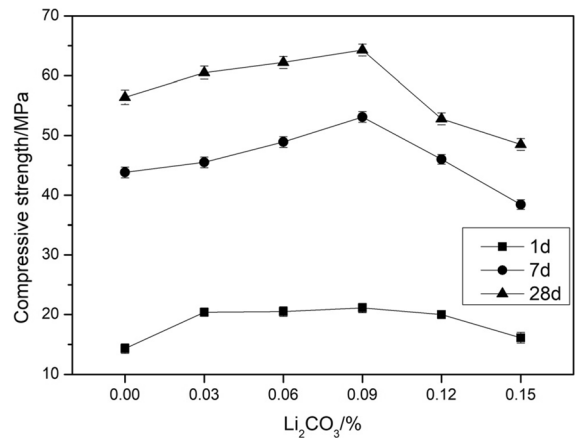
The effect of Li_2CO_3 on the compressive strength of hardened cement paste at 1 day, 7 days and 28 days is presented in Fig. 3. As the content of Li_2CO_3 is increased, the compressive strength is first increased and then decreased. The compressive strength of the hardened paste at 1 day, 7 days, and 28 days reaches the maximum when the content is 0.09 wt%. Compared with the control sample, the strength is increased by 47.6%, 21.2% and 14.0%. The early strength of paste is considerably influenced by Li_2CO_3. The strength at 28 days is changed with the hydration time, but the variation is small. When the dosage is more than 0.09 wt%, it is unfavorable for the strength.

3.3 Hydration heat

The data hydration heat is displayed in Fig. 4. It is observed that the hydration heat of the first exothermal peaks increase after Li_2CO_3 is incorporated, and the
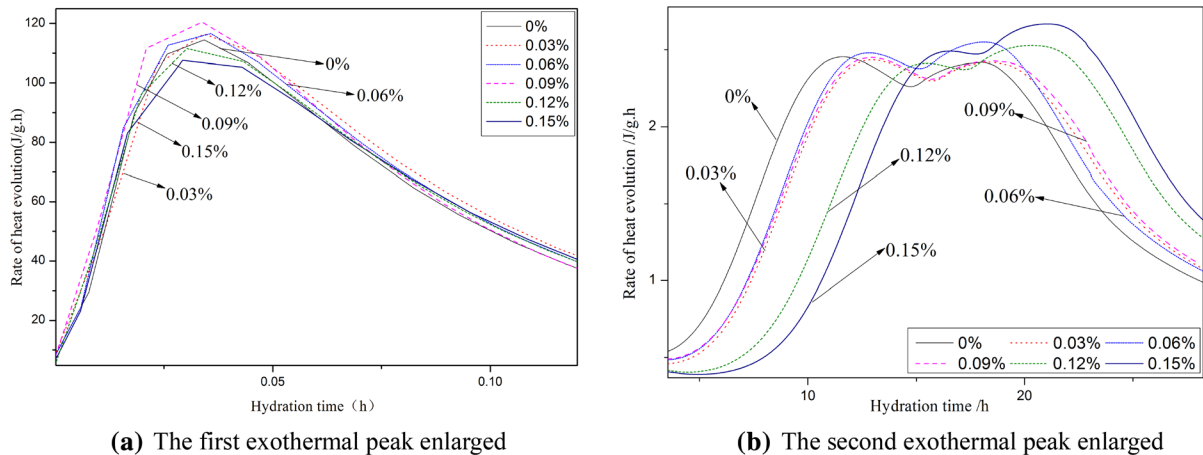
Fig. 3 Effect of Li_2CO_3 on compressive strength of hardened cement paste

peak value of the control sample is 114.3 mW. The peak value reaches the maximum when the content of Li_2CO_3 is 0.09 wt%. It is generally believed that the first exothermal peak is ascribed to the formation of ettringite (AFt), causing induction stage[26, 27], so it can be deduced that Li_2CO_3 has facilitated the formation of AFt.

Figure 4(b) shows that as the content of Li_2CO_3 is increased from 0 to 0.15 wt%, the second exothermal peak shifts right significantly. It is interesting to observe that when the content of Li_2CO_3 is 0.15 wt%, the time for the second exothermal peak appearing has increased by 4.6 h compared with the sample without Li_2CO_3. The second exothermal peak should be ascribed to the hydration of tricalcium silicate (C_3S). Therefore, the incorporation of Li_2CO_3 delays the C_3S hydration, and the more the content is, the more obvious the effect is. However, the peak of the second exothermal peak is slightly larger than that of the control sample, which indicates that although Li_2CO_3 delays the hydration of C_3S, it promotes its hydration degree. This is consistent with the results that the setting of the PC paste was prolonged and the early strength was increased.

A "Peak shoulder" appears after the second exothermal peak, around 18 h, which is caused by the conversion of AFt to AFm [28, 29]. As the ratio of sulfate/aluminate (the mole ratio $\approx$ 3.0) in the liquid phase is high at the start of hydration, the hydrate which first appears is AFt [30, 31]. However, when the sulfate is exhausted, C_3A and C_4AF start to hydrate again, the aluminate concentration in the solution

Fig. 2 pH value of cement pastes with different contents of Li_2CO_3

(a) The first exothermal peak enlarged

(b) The second exothermal peak enlarged

Fig. 4 Exothermal curves of PC pastes with different contents of Li_2CO_3

rises, the ettringite reacts with aluminate to monosulfate [32]. The incorporation of Li_2CO_3 causes the "peak shoulder" to shift to the right. When the content is 0.15wt%, is the "peak shoulder" obviously shifted to the right, at about 3 h. This indicates that Li_2CO_3 can inhibit the conversion of AFt to AFm to some extent.

3.4 TG–DTA

Figure 5 presents the TG–DTA patterns of all the samples. It can be seen that all the DTA patterns consist of three major peaks: (i) the first peak around 100–130 °C, is associated with the dehydration of AFt and C–S–H gel; (ii) the second peak at around 460–480 °C could be due to the decomposition of $Ca(OH)_2$, and (iii) the third peak at about 650–740 °C is related to the decomposition of $CaCO_3$.

In Fig. 5(a), all samples are cured for 1 day. The DTA curves mainly show the endothermic peak of AFt and gel losing bound water, and the endothermic peak of $Ca(OH)_2$ and $CaCO_3$ decomposed by heat. Clearly, when the dosage of Li_2CO_3 is increased from 0 to 0.15 wt%, the mass loss of hydration products between different samples are not significantly different from TG curves, but Li_2CO_3 could promote the hydration of the paste. This result is also in line with the hydration heat.

At 7 days age, in Fig. 5(b), different from the curing for 1 day, the DTA curves show a new endothermic peak at 170–190 °C, which is the process of the AFm losing the bound water when heated. It can

also be seen that when the Li_2CO_3 content is 0.09 wt%, the endothermic peaks of AFt and gel are significantly deeper.

In Fig. 5(c), at 28 days, the changing law of the curves is the same as that of curing for 7 days, and the hydration product remains unchanged. The TG curves show that the mass loss decreases more than the curing 1 day and 7 days. Clearly, as the curing age increases, the hydration of the paste is more sufficient.

In summary, as the Li_2CO_3 content increases from 0 to 0.09 wt%, the endothermic peaks of AFt and $Ca(OH)_2$ change from shallow to deep, and the weight loss rate also increases. Combined with the hydration heat analysis, the pastes of different ages have the highest degree of hydration when the content of Li_2CO_3 is 0.09 wt%. At the same time, there is also an endothermic peak of $CaCO_3$, and a certain amount of $CaCO_3$ makes the hardened paste more dense and advantageous for strength.

3.5 XRD analysis

The XRD patterns are plotted in Fig. 6. For the pastes cured for 1 day, 7 days, or 28 days, the main hydration products identified are AFt, $Ca(OH)_2$, C–S–H gel, $CaCO_3$, and un-hydrated C_3S and C_2S.

Li_2CO_3 can react with $Ca(OH)_2$ in the hydrating paste to form $CaCO_3$, as shown in Eq. 1.

$$Li_2CO_3 + Ca(OH)_2 = CaCO_3 \downarrow + 2LiOH \qquad (1)$$

From Fig. 6(a), at 1 day, the diffraction peaks of C–S–H gel and $CaCO_3$ ($2\theta \approx 29°$) increase as the
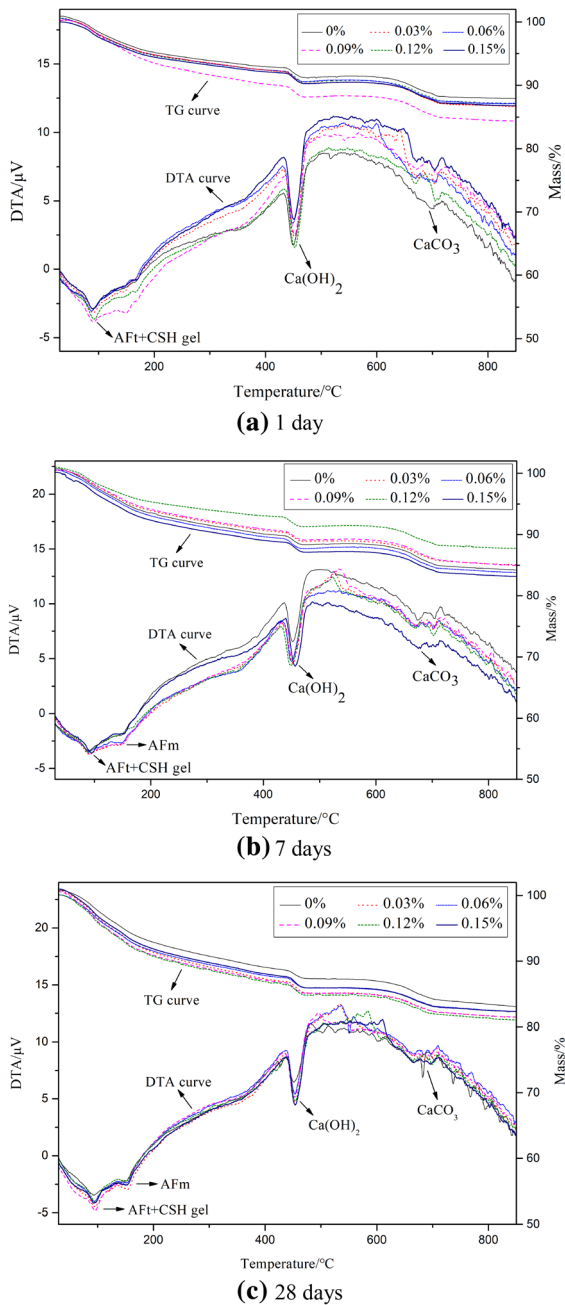
Fig. 5 TG–DTA diagram of the effect of Li_2CO_3 on the cement hydration

content of Li_2CO_3 is increased, indicating that Li_2CO_3 may facilitate the formation of $CaCO_3$. This is confirmed by the TG–DTA results. More $CaCO_3$ formation can fill more pores in the hydrated pastes, so the number of pores may be reduced, leading to an increase in the compressive strength. This further
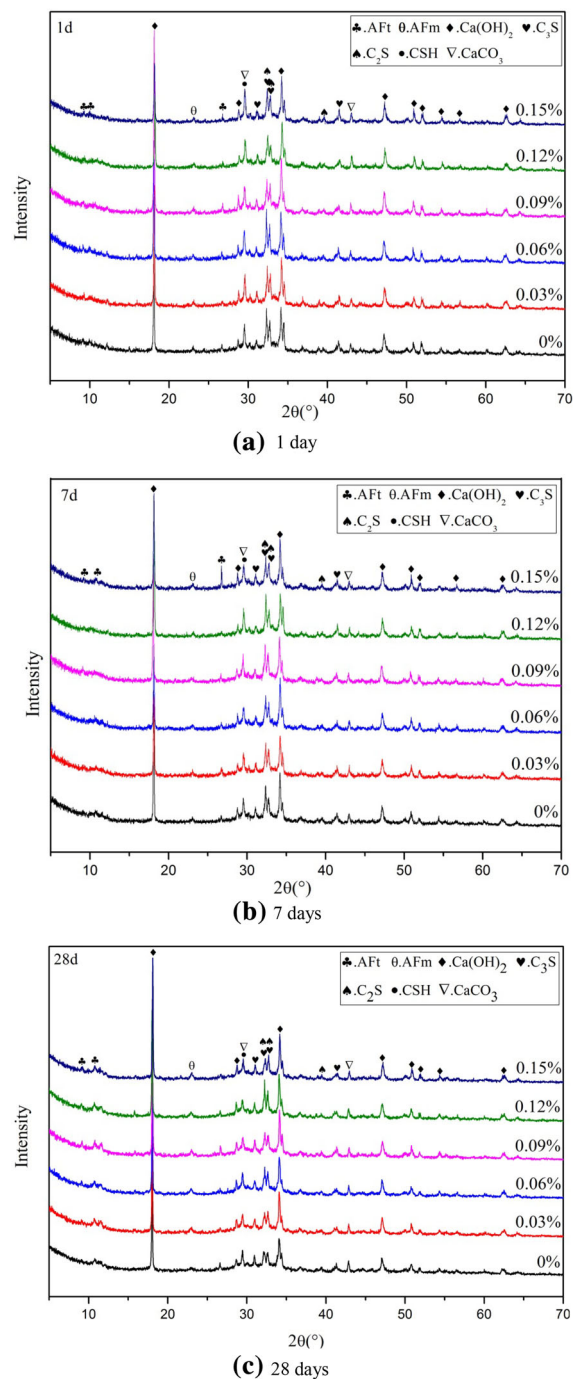
Fig. 6 XRD patterns of PC pastes cured for 1 day, 7 days and 28 days

demonstrates the compressive strength results. From Fig. 6(b), at 7 days, the XRD peaks of C–S–H gel, $CaCO_3$ $(2\theta \approx 29°)$, and $Ca(OH)_2$ $(2\theta \approx 34°)$ increases with the increase of Li_2CO_3 content. This
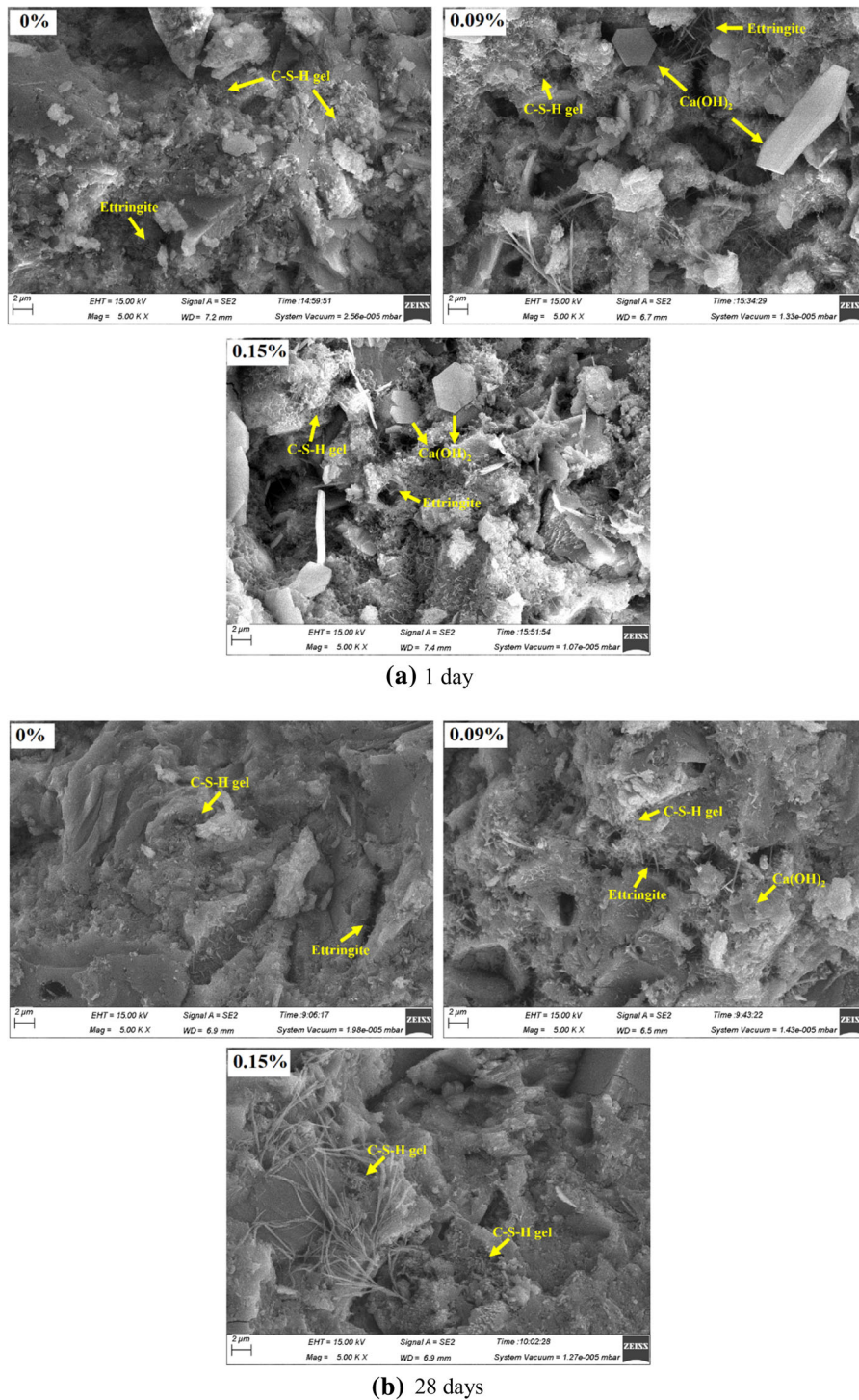
(a) 1 day

(b) 28 days

Fig. 7 SEM image of cement pastes at 1 day and 28 days with different Li_2CO_3 content

may be because the addition of Li_2CO_3 promotes the hydration of C_3S.

In Fig. 6(c), at 28 days, the XRD peak of AFt ($2\theta \approx 9°$) increases with the increase of Li_2CO_3

Table 3 Porosity and pore size distribution of pastes with different Li_2CO_3 content

Content (wt%)	Porosity (%)	Pore size (nm)/(%)			
		< 20	20–100	100–200	> 200
0	18.53	16.28	63.66	7.19	12.87
0.03	16.42	23.07	65.52	5.56	5.85
0.06	16.06	18.61	61.23	10.51	9.65
0.09	15.69	33.80	54.45	5.49	6.56
0.12	17.42	14.11	72.25	3.94	9.70
0.15	16.57	19.65	51.87	14.44	14.04
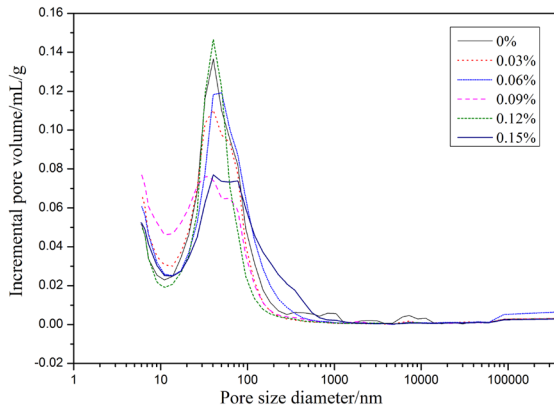
(a) Pore size distribution
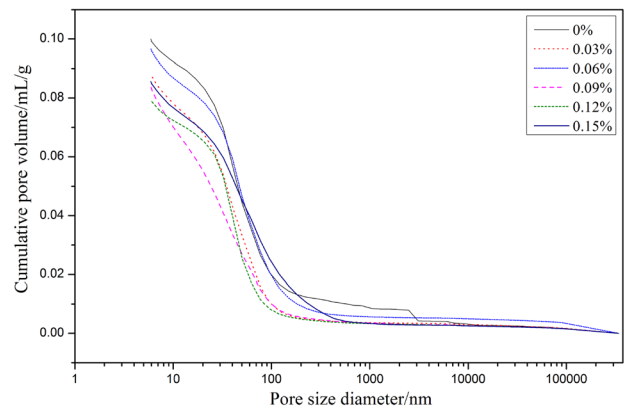
(b) Cumulative pore volume

Fig. 8 Effect of Li_2CO_3 content on the pore structure of pastes

content. This further demonstrates that Li_2CO_3 may promote the formation of ettringite, in line with the previous hydration heat data of AFt. Nevertheless, the change in the peaks of the C–S–H gel is little.

3.6 SEM analysis

Figure 7 presents the SEM images of the cement samples with different contents of Li_2CO_3. In Fig. 7(a), at 1 day, compared to the control sample, in the sample doped with Li_2CO_3, more needle-like AFt crystals and flocculent C–S–H gel are obviously observed. This again demonstrates that the addition of Li_2CO_3 promotes the formation of AFt and C–S–H gels, which is consistent with the XRD results. More pores and cracks can also be observed in the figures, and the structure is relatively loose. In Fig. 7(b), compared with the samples at 1 day, the AFt crystals and C–S–H gel in the samples hydrated for 28 days still exists, which are not obvious enough, but the structure looks more compact.

3.7 Pore structure

The results of the pore structure of the samples subjected to 28-day curing are shown in Table 3 and Fig. 8. It can be seen that as the content of Li_2CO_3 increases, the porosity of the hardened paste first decreases and then increases. When the content of Li_2CO_3 is 0.09 wt%, the porosity is the lowest. Moreover, the diameter of most pores is below 100 nm. In general, the incorporation of Li_2CO_3 increases the ratio of harmless pores (< 20 nm) of the sample, except the content of 0.12 wt%. In particular, when the content is 0.09 wt%, the ratio of harmless pores (< 20 nm) considerably increases compared to the control sample, which is increased by 17.5%. And the ratio of less harmful holes (20–100 nm), harmful holes (100–200 nm) and harmful holes (> 200 nm) are smaller than the control samples, which is reduced by 9.5%, 1.7% and 6.3%. This indicates that the pore size of the harmful pores was optimized when the Li_2CO_3 content is in the range

of 0.06–0.09wt%, increasing the compactness of the paste.

From Fig. 8(a), when the content of Li_2CO_3 is $0 \sim 0.09$wt%, the proportion of harmless pores (< 20 nm) in the hardened paste increases, while the proportion of less harmful holes, harmful holes and harmful holes decrease. When the content is in the range of 0.09–0.15wt%, the regularity of the pore structure is reversed. Compared with the control sample, when the Li_2CO_3 content is 0.09wt%, the porosity of the hardened paste is reduced, the pore size is optimized, and the proportion of macropores (> 20 nm) is reduced. As a result, the compactness of the hardened PC paste is improved. The change of the pores agrees with the change of compressive strength.

4 Conclusion

The influence of different contents of Li_2CO_3 on the hydration and hardening properties of cement paste was studied and then the mechanism analysis was revealed. Therefore, the main conclusions are shown as follows:

(1)　The incorporation of Li_2CO_3 delays the setting of cement pastes. As the content of Li_2CO_3 is between 0.06 and 0.12 wt%, the delaying effect is evident. When the content was 0.09 wt%, the initial setting time and the final setting time are increased by 19.8% and 27.7%.

(2)　As the content of Li_2CO_3 is increased, the compressive strength the hardened PC pastes at 1 day, 7 days and 28 days is increased first and then decreased. The compressive strength reaches the highest value when the content is 0.09 wt%. The compressive strength of the PC pastes at 1 day, 7 days and 28 days is increased by 47.6%, 21.2% and 14%.

(3)　Li_2CO_3 promotes the formation of ettringite and optimizes the microstructure of the hardened pc pastes. As the content of Li_2CO_3 is 0.09 wt%, the porosity of the paste is lowest and the compactness reaches the best.

References

1. Blanc AFC (2000) Setting-retarder and its application to concrete, mortars andor grouts. Cement Concr Compos 22(4):309
2. Ozkul MH (2000) Utilization of citro- and desulphogypsum as set retarders in Portland cement. Cem Concr Res 30(11):1755–1758
3. Massarweh O, Maslehuddin M, Al-Dulaijan SU, Shameem M, Ahmad S (2020) Development of a concrete set retarder utilizing electric arc furnace dust. Constr Build Mater 255:119378
4. Guo P, Zhang Z, Zhang Y, Han F, Shou C (2020) Controllable synthesis of terminal carboxyl hyperbranched polyester and their retarding effect on concrete. J Polym Res 27(8)
5. Afroz S, Manzur T, Anwar Hossain KM (2020) Arrowroot as bio-admixture for performance enhancement of concrete. J Build Eng 30:101313
6. Zajac M, Skocek J, Bullerjahn F, Ben HM (2016) Effect of retarders on the early hydration of calcium-sulpho-aluminate (CSA) type cements. Cem Concr Res 84:62–75
7. Xia X, Guo J, Chen D, Feng Y, Yu Y, Jin J et al (2017) Hydrophobic associated copolymer as a wide temperature range synthetic cement retarder and its effect on cement hydration. J Appl Polym Sci 134(35):e45242
8. Chang JJ, Yeih W, Hung CC (2005) Effects of gypsum and phosphoric acid on the properties of sodium silicate-based alkali-activated slag pastes. Cement Concr Compos 27(1):85–91
9. Hall DA, Stevens R, El-Jazairi B (2001) The effect of retarders on the microstructure and mechanical properties of magnesia-phosphate cement mortar. Cem Concr Res 31(3):455–465
10. Akın Altun İ, Sert Y (2004) Utilization of weathered phosphogypsum as set retarder in Portland cement. Cem Concr Res 34(4):677–680
11. Huang G, Pudasainee D, Gupta R, Liu WV (2020) Utilization and performance evaluation of molasses as a retarder and plasticizer for calcium sulfoaluminate cement-based mortar. Constr Build Mater 243:118201
12. Zhang L, Catalan LJJ, Balec RJ, Larsen AC, Esmaeili HH, Kinrade SD (2010) Effects of saccharide set retarders on the hydration of ordinary portland cement and pure tricalcium silicate. J Am Ceram Soc 93(1):279–287
13. Weifeng LI, Suhua MA, Shengbiao Z, Xiaodong S (2014) Physical and chemical studies on cement containing sugarcane molasses. J Therm Anal Calorim 118(1):83–91
14. Combrinck R, Kayondo M, le Roux BD, de Villiers WI, Boshoff WP (2019) Effect of various liquid admixtures on cracking of plastic concrete. Constr Build Mater 202:139–153
15. Zhu P, Jiang L, Shi Y, Xu N, Jin M (2020) Influence of retarders on hydration and microstructure development of

cement containing high-volume limestone powder. J Therm Anal Calorim 141(2):685–696

16. Lei L, Li R, Fuddin A (2020) Influence of maltodextrin retarder on the hydration kinetics and mechanical properties of Portland cement. Cem Concr Compos 114:103774

17. Ltifi M, Guefrech A, Mounanga P (2011) Effects of sodium tripolyphosphate addition on early-age physic–chemical properties of cement pastes. Proc Eng 10(1):1457–1462

18. Ramachandran VS, Lowery MS, Wise T, Polomark GM (1993) The role of phosphonates in the hydration of Portland cement. Mater Struct 26(7):425–432

19. Kupwade Patil K, Boul PJ, Rasner DK, Lapidus SH, Leao JB, Johnson KD et al (2020) In situ investigation of phosphonate retarder interaction in oil well cements at elevated temperature and pressure conditions. J Am Ceram Soc 103(11):6400–6413

20. Shahzad Q, Wang X, Wang W, Wan Y, Li G, Ren C et al (2020) Coordinated adjustment and optimization of setting time, flowability, and mechanical strength for construction 3D printing material derived from solid waste. Constr Build Mater 259:119854

21. Zhang L, Ji Y, Huang G, Gao F, Dong Z (2019) Effect of borax on early hydration and rheological properties of reactivated cementitious material. Adv Cem Res 31(5):235–242

22. Wang J, Han L, Liu Z, Wang D (2020) Setting controlling of lithium slag-based geopolymer by activator and sodium tetraborate as a retarder and its effects on mortar properties. Cem Concr Compos 110:103598

23. Xu Y, Li P, Liu M, Yu Y, Guo J (2020) Synthesis, performance and working mechanism of a novel amphoteric polycarboxylate dispersant without chlorine ion. Constr Build Mater 247:118613

24. Liu H, Bu Y, Ma R, Guo W (2019) Improve the practicability of calcium aluminate phosphate cement as well cement: the application of amphoteric ion polymer as retarder. Constr Build Mater 199:207–213

25. China SAOT (2011) Test methods for water requirement of normal consistency, setting time and soundness of the Portland cement. GB/T 1346-2011. Beijing: China Architecture & Building Press

26. Xiong Z, Peng W, Wang Y (2015) Hydration behaviors of portland cement with different lithologic stone powders. Int J Concr Struct Mater 9(1):55–60

27. Barnes P (2003) Structure and performance of cements. Spon Press, London

28. Yuli W, Fengxia H, Lei Y (2018) Influence of dry ice on the performance of Portland cement and its mechanism. Constr Build Mater 188:898–904

29. Bullard JW, Jennings HM, Livingston RA, Nonat A, Scherer GW, Schweitzer JS et al (2011) Mechanisms of cement hydration. Cem Concr Res 41(12):1208–1223

30. Zhang S, Xu X, Memon SA, Dong Z, Li D, Cui H (2018) Effect of calcium sulfate type and dosage on properties of calcium aluminate cement-based self-leveling mortar. Constr Build Mater 167:253–262

31. Wang Y, He H, He F (2018) Effect of slaked lime and aluminum sulfate on the properties of dry-mixed masonry mortar. Constr Build Mater 180:117–123

32. Aitcin PC (2006) Concrete structure, properties and materials. Preticehall Int 13(4):499